

Nonlinear Model Updating of Geometrically Nonlinear Structures based on Gaussian Process Regression Reduced Order Modeling

Kyusic Park¹ and Matthew S. Allen²

¹ University of Minnesota - Department of Aerospace Engineering and Mechanics,

² Brigham Young University - Department of Mechanical Engineering
email: kpark26@umn.edu, matt.allen@byu.edu

Abstract

Finite element model updating (FEMU) seeks to tie simulations of digital twin models to the actual performance of the geometrically nonlinear structure of interest. Recently developed FEMU methods have adopted nonlinear responses (e.g., nonlinear normal modes) as a correlation metric, which provides strong assurance of agreement between the model and the actual structure of interest, but is expensive as it requires an iterative computation of the nonlinear response of the FEM as adjustments are made. Reduced order models (ROMs) can be an effective alternative to the full-order FEMs to dramatically reduce the cost of computing the nonlinear responses, but they are typically only valid for a single FEM configuration and must be recomputed if the model is updated. This study presents a novel model updating approach that incorporates a data-driven ROM trained by Gaussian Process regression (i.e., GPR ROM) into the model updating procedure. The GPR ROM is trained with FEMs with varying design parameters, and thus is capable of capturing design variation in FEM. That is, for a given set of FEM parameters within the trained range, the GPR ROM can immediately produce a nonlinear modal model in the form of a non-intrusive ROM, such as implicit condensation and expansion (ICE) ROM. In the proposed model updating routine, when given an initial guess of unknown FEM parameters, the GPR ROM quickly predicts a corresponding ICE ROM for the initial FEM parameters, and the ICE ROM is used to compute and compare the nonlinear normal modes (NNMs) to the target NNMs. The GPR ROM also provides the analytical gradient of the NNMs with respect to the FEM parameters and this is effectively used to find new FEM parameters that improve agreement between the simulated and target NNMs. In this work, a numerical example of a flat beam model is studied to validate the effectiveness of the proposed model updating approach.

Keywords: Nonlinear Dynamics, Geometric Nonlinearity, Finite Element Model Updating, Data-driven Reduced Order Modeling, Gaussian Process Regression

1 Introduction

Finite element model (FEM) has served as an effective and cost-saving digital twin to virtually represent the geometrically nonlinear structures, which typically comprise the skin panels of advanced air vehicles [1–4]. As the advanced vehicles experience extreme flight conditions such as thermal, acoustic and aerodynamic stresses [5–7], a FEM or a digital twin should be able to accurately simulate highly nonlinear responses and stresses of an actual thin structure. This is a difficult task in practice because some discrepancies exist between the digital twin and the actual structure in terms of geometry, material properties and boundary conditions. Thus, the FEM parameters need to be well correlated and updated to minimize the gaps between the simulated predictions and the experimental measurements of an actual structure.

Model correlation and updating methods have been investigated with a significant amount of attention over the past few decades [8, 9]. A majority of existing methods utilize the linear modal properties of a structure to correlate between FE predictions and physical observations. The most common metrics used are natural frequencies and mode shapes, which are load invariant and easily computed from both FEM and experiments [10–12]. One main limitation of linear model correlation is that its approximation is only valid for small deformations from the equilibrium. Once the structure’s behavior deviates far from the linear range, the linear approach may at most provide roughly conservative solutions that cannot explain the nonlinearity. Thus, it is gaining more importance for the model correlation and updating to account for the nonlinearity of structures due to large deformations.

Nonlinear model updating based on FEM has been recently studied by several groups [13–15]. The studies revealed that FEM updating (FEMU) could be accurately achieved by directly updating the FEM parameters to match the simulated

nonlinear responses to the experimentally measured data. In particular, these studies used nonlinear normal modes (NNMs) as the nonlinear responses to be correlated, which have been known as an efficient response metric due to their temporal and spatial independence from applied forcing and also their easy-to-measure characteristics [16–19]. Although the direct FEMU methods provide accurate results, the computational cost required for the procedure becomes a critical issue. For example, when the NNMs are used in the updating procedure, the backbone curves and their numerical gradients with respect to FEM parameters are iteratively computed for making changes to the parameters. This results in a prohibitive computational overhead for the FEMU as the number of FEM elements becomes large.

This issue can be alleviated by substituting the full-order FEM with its reduced order model (ROM) for the model updating. Reduced order modeling significantly reduces the cost of computing nonlinear responses by projecting the full-order equations of motions of the FEM onto a reduced subset of the modal basis. Various non-intrusive ROM methods have been studied and introduced for decades, including stiffness evaluation procedure [20, 21], implicit condensation [22–25], modal derivative [26, 27] and invariant manifold methods [28–31]. For more detailed information, the readers are referred to the recent review papers by Mignolet et al. [32] and Touze et al. [33]. The benefits of applying ROMs to model updating were recently demonstrated by Denis et al. [34], where they used a ROM of normal form and identified its linear and cubic coefficients by correlating the NNM curves of the ROM to experimental data. It was shown in their circular plate example that a single-DOF ROM could accurately correlate the plate model to match the measured experimental backbone curve. ROM updating has also been developed recently by VanDamme et al. [35], where they derived an analytical sensitivity of NNMs with respect to the ROM coefficients when the NNMs were computed by the multi-harmonic balance (MHB) method. They tested the approach on a 3D printed curved beam example and showed that the analytical gradients further improve the computational efficiency of the updating procedure and also provide an accurate correlation.

Despite the significant computational advancement, there are some critical drawbacks of ROMU approaches. One is that a ROM has redundant design variables to correlate in the model updating procedure. For example, as the number of modes increases in a ROM of cubic-order nonlinearity, the number of nonlinear coefficients increases quartically. Because the nonlinear coefficients act as the design variables in the updating routine, using too many nonlinear coefficients in a multi-mode ROM increases the possibility of converging to a local minimum and also results in poor computational efficiency. Another issue is that the updated ROM from ROMU cannot correctly pass the updated modal information to its parent FEM in the physical domain. One of the author's recent studies investigated a method to directly correlate FEM parameters to the updated ROM and showed successful results in a simple numerical case [36]. However, the algorithm failed to converge to the correct solution when direct correlation was used in more complicated examples (e.g., tuning FEM parameters of a few thin curved structures to match multi-DOF ROM). The main reason was that the problem was poorly posed: each ROM coefficient had been updated independently regardless of their correlation to the FEM parameters, so the updated ROM coefficients often could not be led to a unique/valid FEM solution. The study suggested that the ROM-based approaches may not be reliable in identifying the actual physical parameters in the FEM that need to be updated to match the actual structural design, which is often a fundamental goal of model updating.

This work demonstrates a novel data-driven ROM based model updating approach, which overcomes these challenges arising from both FEMU and ROMU. The authors recently introduced a data-driven ROM of geometrically nonlinear structures in [37], where the ROM was trained by Gaussian process regression (GPR) with a collection of FEMs with varying design parameters. The GPR-based data-driven ROM (GPR ROM) could accurately capture the design variation in the FEM. That is, for making any change of FEM parameters, the GPR ROM can immediately produce a corresponding ROM without any static analysis and Galerkin projection of the FEM. Thus, the data-driven ROM can be efficiently incorporated into the model updating routine to quickly update the FEM parameters to match experimental measurements based on ROM-based simulation.

In this work, a GPR ROM is trained for a range of uncertain FEM parameters and used in the proposed model updating framework. When an initial guess of the FEM parameters is provided, the GPR ROM immediately produces a corresponding implicit condensation and expansion (ICE) ROM. Then, the ICE ROM is used to compute and compare NNMs with target NNMs. The gradients of the NNMs with respect to the FEM parameters are then computed and used to find new FEM parameters that improve the agreement between the simulated and target NNMs.

Adopting a GPR ROM into the model updating framework greatly enhances the computational efficiency of the iterative procedure, thanks to providing the online ROM prediction and ROM-based response (NNMs) computation for any given set of FEM parameters. Also, the GPR ROM provides an analytical sensitivity of the ROM with respect to the FEM. This can be combined with the analytical sensitivity of NNM with respect to ROM, derived in [35], to establish a fully analytical sensitivity between the NNM and FEM. Compared to the conventional FEMU approaches that compute numerical gradients using finite difference methods [38], the proposed method can compute the gradients in a much more robust and fast manner.

The following section outlines an overview of the GPR ROM based model updating framework. A derivation of the analytical sensitivity of the NNMs with respect to the FEM parameters is discussed. Then in Section 3, the proposed model updating framework is tested on a numerical example of a flat beam, where initially guessed FEM parameter sets are updated

to match a simulated target NNM. The paper concludes with a discussion and future work in Section 4.

2 Theory

2.1 GPR ROM for Model Updating of Geometrically Nonlinear Structures

A Gaussian Process regression ROM (GPR ROM) is trained for a collection of varying FEMs of geometrically nonlinear structures to be used in the model updating task. The training framework of GPR ROM was thoroughly introduced in [37], where the reader can find more details. This section briefly recapitulates the formulation and training of GPR ROM for geometrically nonlinear structures.

2.1.1 Reduced Order Modeling of Geometrically Nonlinear Structures

An n -DOF geometrically nonlinear finite element model, parameterized by the d -dimensional FEM parameter set $\mathbf{p} \in \mathbb{R}^d$, can be expressed by the FE equations of motion:

$$\mathbf{M}(\mathbf{p})\ddot{\mathbf{x}} + \mathbf{C}(\mathbf{p})\dot{\mathbf{x}} + \mathbf{K}(\mathbf{p})\mathbf{x} + \mathbf{f}_{\text{nl}}(\mathbf{x}, \mathbf{p}) = \mathbf{f}_{\text{ext}}(t) \quad (1)$$

where \mathbf{x} is the $n \times 1$ displacement, \mathbf{M} , \mathbf{C} and \mathbf{K} are the $n \times n$ mass, damping and stiffness matrices, \mathbf{f}_{nl} is the $n \times 1$ nonlinear restoring forces and \mathbf{f}_{ext} is the $n \times 1$ external forces. The FE equations can be projected to a set of modal basis, defined as

$$(\mathbf{K}(\mathbf{p}) - \omega_r^2(\mathbf{p})\mathbf{M}(\mathbf{p}))\Phi_r(\mathbf{p}) = 0 \quad (2)$$

where ω_r and Φ_r are the r -th linear frequency and $n \times 1$ mass normalized mode shape, respectively. The full-order FE equations in Eq. (1) can be approximated by a linear combination of a reduced set of modal basis $m \ll n$ as

$$\mathbf{x}(t) = \Phi(\mathbf{p})\mathbf{q}(t) \quad (3)$$

where Φ is the $n \times m$ mode shape matrix and \mathbf{q} is the $m \times 1$ modal coordinates. The nonlinear modal equations of motion can be defined by plugging Eq. (3) into Eq. (1) and pre-multiplying by Φ^T . Then the r -th nonlinear modal equation can be expressed as

$$\ddot{q}_r + c_r(\mathbf{p})\dot{q}_r + \omega_r^2(\mathbf{p})q_r + \theta_r(q_1, q_2, \dots, q_m, \mathbf{p}) = \Phi_r(\mathbf{p})^T \mathbf{f}(t) \quad (4)$$

where θ_r is the nonlinear modal restoring force. The modal restoring force θ_r is described by a third-order polynomial in terms of geometric nonlinearity and can be written as

$$\theta_r(q_1, q_2, \dots, q_m, \mathbf{p}) = \sum_{i=1}^m \sum_{j=i}^m \alpha_r(i, j, \mathbf{p})q_iq_j + \sum_{i=1}^m \sum_{j=i}^m \sum_{k=j}^m \beta_r(i, j, k, \mathbf{p})q_iq_jq_k \quad (5)$$

where α_r and β_r are the quadratic and cubic stiffness coefficients. In this work, a ROM defined by Eq. (4) and Eq. (5) is computed using the implicit condensation and expansion (ICE) method [25], which applies a set of prescribed static loads onto the FEM and computes the nonlinear stiffness coefficients in Eq. (5) with the resulting static load-displacement data. The prescribed force set \mathbf{F}_p is defined as

$$\mathbf{F}_p = \mathbf{M}(\Phi_1c_1 + \Phi_2c_2 + \dots + \Phi_mc_m) \quad (6)$$

where c_r is the r -th modal forcing coefficient characterizing the degree of forcing. c_r is further controlled by the force scaling factor f_r as

$$c_r = \frac{f_r}{\Phi_{r,\text{max}}} \omega_r^2 \quad (7)$$

where $\Phi_{r,\text{max}}$ is the entry of the DOF in the r -th mode shape at which the deformation is maximum. The minimum number of static load cases required for the ICE method is the same as the number of nonlinear coefficients per mode in an ICE ROM, which can be written as

$$N_{\text{nl}} = m + m^2 + \frac{m!}{2!(m-2)!} + \frac{m!}{3!(m-3)!} \quad (8)$$

When damping is not considered, an ICE ROM can be represented by a matrix consisting of linear and nonlinear stiffness coefficients:

$$\mathbf{Y} = \begin{bmatrix} \omega_1 & \alpha_1(1,1) & \alpha_1(1,2) & \cdots & \alpha_1(m,m) & \beta_1(1,1,1) & \beta_1(1,1,2) & \cdots & \beta_1(m,m,m) \\ \omega_2 & \alpha_2(1,1) & \alpha_2(1,2) & \cdots & \alpha_2(m,m) & \beta_2(1,1,1) & \beta_2(1,1,2) & \cdots & \beta_2(m,m,m) \\ \cdots & \cdots & \cdots & \cdots & \cdots & \cdots & \cdots & \cdots & \cdots \\ \omega_m & \alpha_m(1,1) & \alpha_m(1,2) & \cdots & \alpha_m(m,m) & \beta_m(1,1,1) & \beta_m(1,1,2) & \cdots & \beta_m(m,m,m) \end{bmatrix} \quad (9)$$

2.1.2 GPR ROM Training

A GPR ROM is a data-driven ROM, which trains each coefficient in an ICE ROM as a non-parametric regression model. A collection of N_{tr} input FEMs is drawn from a random distribution, i.e., $\mathbf{P}_{\text{tr}} = [\mathbf{p}_1, \mathbf{p}_2, \dots, \mathbf{p}_{N_{\text{tr}}}]^T \in \mathbb{R}^{N_{\text{tr}} \times d}$, each of which is formulated based on the FE equations of motion in Eq. (1) with a different parameter vector $\mathbf{p} = [p_1, p_2, \dots, p_d]^T \in \mathbb{R}^d$. The random FEM parameter set \mathbf{p} in the GPR ROM will serve as a design variable set to be optimized in the proposed model updating task.

Each of the FEM samples is applied by the ICE method to compute a corresponding ICE ROM, and the resulting collection of the ROMs can be represented as $\mathbf{Y}_{\text{tr}} = [\mathbf{Y}_1, \mathbf{Y}_2, \dots, \mathbf{Y}_{N_{\text{tr}}}]^T \in \mathbb{R}^{N_{\text{tr}} \times (m \times (N_{\text{nl}} + 1))}$, where \mathbf{Y}_i denotes the i -th ROM's coefficient matrix in Eq. (9). Then for any ROM coefficient $y \in \mathbf{Y}$, its training set can be denoted as $\mathbf{y}_{\text{tr}} = [y_1, y_2, \dots, y_{N_{\text{tr}}}]^T \in \mathbb{R}^{N_{\text{tr}} \times 1}$.

The ROM coefficient y can be described by a Gaussian Process (GP) model in terms of FEM parameters \mathbf{p} , by training $\mathbf{P}_{\text{tr}} - \mathbf{y}_{\text{tr}}$ sample set. The GP model can be written as

$$y(\mathbf{p}) \sim \mathcal{GP}(\eta, \kappa) + \epsilon_n, \quad \epsilon_n \sim \mathcal{N}(0, \sigma_n^2) \quad (10)$$

where \mathcal{GP} implies that the distribution of the ROM coefficient y obeys a Gaussian Process, and η and κ are the mean and covariance functions specifying the Gaussian Process. ϵ_n is an independent noise, which is assumed to follow a normal distribution with variance σ_n^2 . In this study, the mean function of the GP model is constant, $\eta = \eta_m$, and the covariance function κ is the automatic relevance determination squared exponential (ARD SE) kernel [39]:

$$\kappa(\mathbf{p}_i, \mathbf{p}_j) = \sigma_f^2 \exp\left(-\frac{1}{2} \sum_{k=1}^d \frac{(p_{i,k} - p_{j,k})^2}{l_k^2}\right) \quad (11)$$

where $p_{i,k}$ is the k -th parameter of \mathbf{p}_i , σ_f is the output standard deviation, and l_k is the k -th individual length scale.

The GP model y in Eq. (10) can be trained by optimizing its hyperparameters $\boldsymbol{\theta}_h = \{\eta_m, \sigma_f, l_1, l_2, \dots, l_d, \sigma_n\}$ using the maximum likelihood estimation of the sample distribution [40]:

$$\boldsymbol{\theta}_h = \underset{\boldsymbol{\theta}_h}{\operatorname{argmax}} \log p(\mathbf{y}_{\text{tr}} | \mathbf{P}_{\text{tr}}) = \underset{\boldsymbol{\theta}_h}{\operatorname{argmax}} \left(-\frac{1}{2} \log |\boldsymbol{\Sigma}(\boldsymbol{\theta}_h)| - \frac{1}{2} (\mathbf{y}_{\text{tr}} - \boldsymbol{\mu}(\boldsymbol{\theta}_h))^T \boldsymbol{\Sigma}^{-1}(\boldsymbol{\theta}_h) (\mathbf{y}_{\text{tr}} - \boldsymbol{\mu}(\boldsymbol{\theta}_h)) - \frac{N_{\text{tr}}}{2} \log(2\pi) \right) \quad (12)$$

where $\boldsymbol{\mu}(\boldsymbol{\theta}_h)$ is the $N_{\text{tr}} \times 1$ mean vector of $\mu_i(\boldsymbol{\theta}_h) = \eta_m$, and $\boldsymbol{\Sigma}(\boldsymbol{\theta}_h)$ is the $N_{\text{tr}} \times N_{\text{tr}}$ covariance matrix of $\Sigma_{ij}(\boldsymbol{\theta}_h) = \kappa(\mathbf{p}_i, \mathbf{p}_j) + \sigma_n^2 \delta_{ij}$ (where δ_{ij} is the Kronecker delta).

The GPR ROM completes the training as all the coefficients in the ROM matrix \mathbf{Y} are trained as the GP models. Then, for any new design parameter set(s) \mathbf{P}_{te} within the trained range, the corresponding ICE ROM(s) can be quickly predicted with its mean and confidence interval. That is, the conditional mean and covariance of the new test set \mathbf{y}_{te} can be estimated based on the assumption that the training set \mathbf{y}_{tr} and test set \mathbf{y}_{te} follow a joint normal distribution:

$$\mathbf{y}_{\text{te}} | \mathbf{P}_{\text{te}}, \mathbf{P}_{\text{tr}}, \mathbf{y}_{\text{tr}} \sim \mathcal{N}(\boldsymbol{\mu}_* + \boldsymbol{\Sigma}_*^T \boldsymbol{\Sigma}^{-1}(\mathbf{y}_{\text{tr}} - \boldsymbol{\mu}), \boldsymbol{\Sigma}_{**} - \boldsymbol{\Sigma}_*^T \boldsymbol{\Sigma}^{-1} \boldsymbol{\Sigma}_*), \quad (13)$$

where $\boldsymbol{\mu}_*$ is the mean of the test set ($\boldsymbol{\mu}_* = \boldsymbol{\mu}$ in this work because they are constant), $\boldsymbol{\Sigma}_*$ is the training-test set covariance $\kappa(\mathbf{P}_{\text{tr}}, \mathbf{P}_{\text{te}})$ and $\boldsymbol{\Sigma}_{**}$ is the test set covariance $\kappa(\mathbf{P}_{\text{te}}, \mathbf{P}_{\text{te}})$.

2.2 GPR ROM based Model Updating

2.2.1 Proposed Model Updating Framework

The flowchart of the proposed GPR ROM based model updating method is shown in Figure 1. First, the lower and upper bounds of uncertain design parameters ($\mathbf{p}_{\text{min}}, \mathbf{p}_{\text{max}}$) are defined and an initial guess of the design parameter set \mathbf{p}_0 is provided. Then, the framework trains a GPR ROM with uniformly sampled FEMs within the parameter range. The GPR ROM generates an ICE ROM for the initial guess \mathbf{p}_0 , and the ICE ROM is used to compute a nonlinear normal mode (NNM) backbone curve of the initial structural model. The numerical NNM is compared with the target NNM (e.g., experimental data) and their gap can be minimized by an iterative procedure of updating the FEM parameters, predicting the ICE ROM from the GPR ROM, and computing the updated NNM. The design sensitivity of NNM with respect to the FEM parameters determines the next estimate of the FEM parameters. The sensitivity analysis will be discussed in the following section.

In this work, NNMs are computed by applying the multi-harmonic balance (MHB) method [41]. The MHB method is beneficial to be used in this proposed model updating routine, because it provides analytical gradients of the NNMs with respect to the ICE ROM as shown in [35].

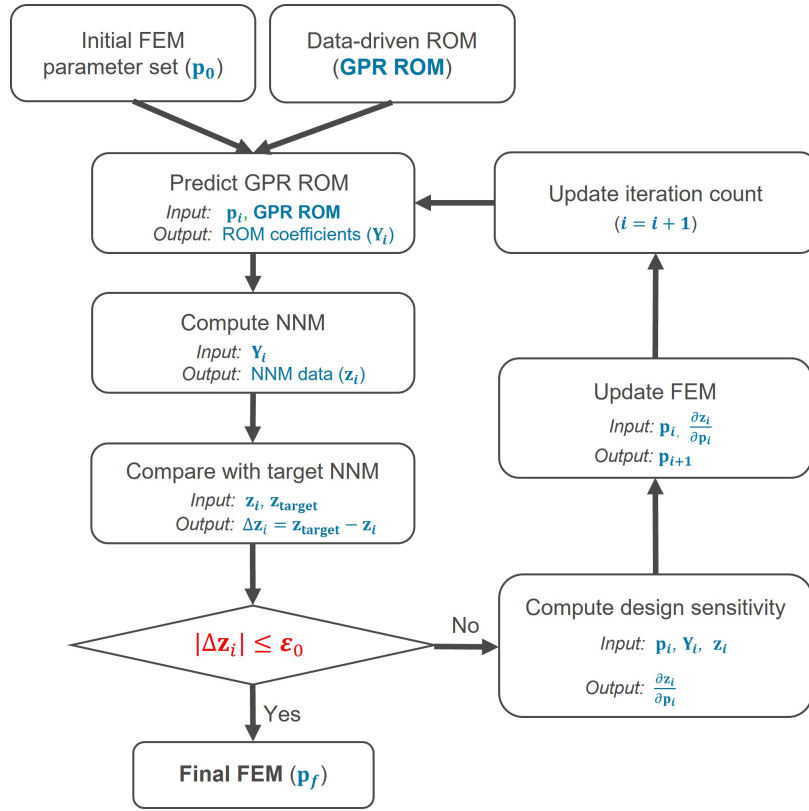


Figure 1: Flowchart of the proposed GPR ROM based model updating framework.

The model updating framework aims to minimize the discrepancy between the numerical and target NNMs by adjusting the FEM parameters. The objective function to be minimized is formulated in a quadratic form:

$$\Gamma = \Delta \mathbf{z}^T \mathbf{W}_z \Delta \mathbf{z} + \gamma \Delta \mathbf{p}^T \mathbf{W}_p \Delta \mathbf{p} \quad (14)$$

where \mathbf{z} is the vector of state variables. The state variables are the values of the NNM at different amplitudes, and $\Delta \mathbf{z}$ is the distance between each point on the NNM from the ROM and the target or measured NNM. γ is the weighting term to control the effect of the second term (changes in the design variables) with respect to the first term (a gap between the state variables and the target variables). \mathbf{W}_z and \mathbf{W}_p are weighting matrices governing the relative weights between the different state and design variables, respectively. In this work these matrices are identity matrices, meaning that each term in each vector is weighted equally. Minimizing the cost function leads to achieving the minimum discrepancy between the updated and target NNM, while constraining the change in the design parameters to be minimal.

The state variable error vector $\Delta \mathbf{z}$ is defined by the Euclidean distance between each target NNM point and its closest numerical NNM point on the 2D frequency-amplitude plane. Note that the amplitude on the plane can be defined by either physical or modal displacement of a node of interest, and the Euclidean distance is computed with normalized frequency and amplitude. The optimization routine finds the minimum objective function based on a gradient-based method, i.e., the interior-point algorithm [42], implemented in the MATLAB[®] built-in function *fmincon*.

2.2.2 Design sensitivity analysis

The computational efficiency of minimizing the cost function in Eq. (14) is determined by how the design sensitivity of the state variables with respect to the design variables is formulated. For example, if the design sensitivity were computed numerically by finite difference methods, it would require a significantly increased number of NNM computations, and the resulting gradients could be affected by possible numerical errors.

The proposed GPR ROM based model updating enables to compute a fully analytical design sensitivity of the NNMs with respect to the FEM parameters, which can be defined as

$$\frac{\partial \mathbf{z}}{\partial \mathbf{p}} = \frac{\partial \mathbf{z}}{\partial \mathbf{Y}} \frac{\partial \mathbf{Y}}{\partial \mathbf{p}} \quad (15)$$

The first term $\frac{\partial \mathbf{z}}{\partial \mathbf{Y}}$ is the design sensitivity of the NNMs (\mathbf{z}) with respect to the ROM coefficient matrix (\mathbf{Y}). The sensitivity matrix has the size of $N_z \times N_{\text{nl}}$, where N_z is the number of the NNM points used as the state variables. This work uses the analytically derived NNM-to-ROM sensitivity $\frac{\partial \mathbf{z}}{\partial \mathbf{Y}}$ based on the algebraic equations of the MHB method, which was recently derived by VanDamme et al. The detailed derivation can be found in [35].

The second sensitivity term $\frac{\partial \mathbf{Y}}{\partial \mathbf{p}}$ linking the FEM and ROM can be derived based on the GPR ROM equations. As shown in Eq. (13), the trained GPR ROM provides a mean prediction of the ROM coefficient $\bar{y}(\mathbf{p})$ for a given FEM parameter set \mathbf{p} :

$$\bar{y}(\mathbf{p}) = \mu_*(\mathbf{p}) + \Sigma_*^T(\mathbf{p})\Sigma_*^{-1}(\mathbf{y}_{\text{tr}} - \boldsymbol{\mu}) \quad (16)$$

In this work, $\mu_* = \mu_m$ is constant and so only the covariance term of the training-test set $\Sigma_*(\mathbf{p})$ changes as the FEM parameters are varied. Then, the derivative of the mean prediction can be defined as

$$\frac{\partial \bar{y}(\mathbf{p})}{\partial \mathbf{p}} = \frac{\partial \Sigma_*^T(\mathbf{p})}{\partial \mathbf{p}} \Sigma_*^{-1}(\mathbf{y}_{\text{tr}} - \boldsymbol{\mu}) \quad (17)$$

The derivative of the covariance term can be expressed as

$$\frac{\partial \Sigma_*(\mathbf{p})}{\partial \mathbf{p}} = \begin{bmatrix} \frac{\partial \kappa_{1*}}{\partial \mathbf{p}} & \frac{\partial \kappa_{2*}}{\partial \mathbf{p}} & \dots & \frac{\partial \kappa_{N_{\text{tr}}*}}{\partial \mathbf{p}} \end{bmatrix}^T \quad (18)$$

where κ_{i*} is the trained GP covariance function, defined as

$$\begin{aligned} \kappa_{i*} &= \kappa(\mathbf{p}_{\text{tr},i}, \mathbf{p}) = \sigma_f^2 \exp\left(-\frac{1}{2}(\mathbf{p}_{\text{tr},i} - \mathbf{p})^T \boldsymbol{\Lambda}^{-1}(\mathbf{p}_{\text{tr},i} - \mathbf{p})\right) \\ &= \sigma_f^2 \exp\left(-\frac{1}{2} \sum_{k=1}^d \frac{((p_k)_{\text{tr},i} - p_k)^2}{l_k^2}\right) \end{aligned} \quad (19)$$

where $\boldsymbol{\Lambda}$ is the diagonal matrix of the individual length scales, i.e., $\boldsymbol{\Lambda} = \text{diag}(l_1^2, l_2^2, \dots, l_d^2)$. The derivative of the covariance function can be derived as

$$\begin{aligned} \frac{\partial \kappa_{i*}}{\partial \mathbf{p}} &= \frac{\partial}{\partial \mathbf{p}} \left[\sigma_f^2 \exp\left(-\frac{1}{2}(\mathbf{p}_{\text{tr},i} - \mathbf{p})^T \boldsymbol{\Lambda}^{-1}(\mathbf{p}_{\text{tr},i} - \mathbf{p})\right) \right] \\ &= \boldsymbol{\Lambda}^{-1}(\mathbf{p}_{\text{tr},i} - \mathbf{p}) \kappa_{i*} \end{aligned} \quad (20)$$

The derivative of the mean prediction of the ROM coefficient in Eq. (17) can then be rewritten as

$$\begin{aligned} \frac{\partial \bar{y}(\mathbf{p})}{\partial \mathbf{p}} &= \boldsymbol{\Lambda}^{-1} \begin{bmatrix} (\mathbf{p}_{\text{tr},1} - \mathbf{p}) \kappa_{1*} & (\mathbf{p}_{\text{tr},2} - \mathbf{p}) \kappa_{2*} & \dots & (\mathbf{p}_{\text{tr},N_{\text{tr}}} - \mathbf{p}) \kappa_{N_{\text{tr}}*} \end{bmatrix} \Sigma_*^{-1}(\mathbf{y}_{\text{tr}} - \boldsymbol{\mu}) \\ &= \boldsymbol{\Lambda}^{-1} \left[(\mathbf{P}_{\text{tr}}^T - \mathbf{p} \mathbf{1}_{N_{\text{tr}}}^T) \text{diag}(\Sigma_*(\mathbf{p})) \right] \Sigma_*^{-1}(\mathbf{y}_{\text{tr}} - \boldsymbol{\mu}) \end{aligned} \quad (21)$$

where $\mathbf{1}_{N_{\text{tr}}}$ is the $N_{\text{tr}} \times 1$ vector of all ones. Then, the derivative of the ROM coefficient matrix with respect to a given FEM parameter set can be defined as

$$\begin{aligned} \frac{\partial \mathbf{Y}(\mathbf{p})}{\partial \mathbf{p}} &\approx \frac{\partial \bar{\mathbf{Y}}(\mathbf{p})}{\partial \mathbf{p}} = \begin{bmatrix} \frac{\partial \bar{y}_1(\mathbf{p})}{\partial \mathbf{p}} & \frac{\partial \bar{y}_2(\mathbf{p})}{\partial \mathbf{p}} & \dots & \frac{\partial \bar{y}_{N_{\text{nl}}}(\mathbf{p})}{\partial \mathbf{p}} \end{bmatrix}^T \\ &= \begin{bmatrix} \frac{\partial \bar{\omega}_1(\mathbf{p})}{\partial \mathbf{p}} & \frac{\partial \bar{\omega}_2(\mathbf{p})}{\partial \mathbf{p}} & \dots & \frac{\partial \bar{\beta}_m(m, m, m)(\mathbf{p})}{\partial \mathbf{p}} \end{bmatrix}^T \end{aligned} \quad (22)$$

whose size is $N_{\text{nl}} \times d$. The gradient $\frac{\partial \mathbf{Y}}{\partial \mathbf{p}}$ can be pre-multiplied by the gradient of the NNMs to the ROM $\frac{\partial \mathbf{z}}{\partial \mathbf{Y}}$ to achieve the fully analytical gradient $\frac{\partial \mathbf{z}}{\partial \mathbf{p}}$ in Eq. (15). Note that the size of the final design sensitivity matrix is $N_z \times d$.

3 Numerical Study - Flat Beam

The proposed procedure was tested numerically on the flat beam finite element model, which was previously studied in [37]. The beam model with axial boundary springs is shown in Figure 2. The nominal beam had a length of 228.6 mm, a width of 12.7 mm, and a thickness of 0.787 mm. The material properties followed the nominal values of steel where the mass density was 7800 kg m^{-3} , Young's modulus was 206.84 GPa, and Poisson's ratio was 0.29. The beam model was composed of 40 2-node beam elements.

The boundary stiffness K_x was chosen as a design variable for the model updating, because this parameter is typically computed to approximate the effect of the boundary conditions and hence can be highly uncertain. In this case study, the boundary stiffness was assumed to be within the bounds of $[K_{x,\min}, K_{x,\max}] = [1.0 \times 10^4, 5.0 \times 10^5] \text{ lbf in}^{-1}$, which could represent soft to nearly clamped boundary stiffness.

3.1 GPR ROM of Flat Beam

As the first step of the model updating procedure, a GPR ROM could be trained that allows K_x to vary within those bounds. Some important GPR ROM training parameters were defined and are presented in Table 1. The GPR ROM was trained using 20 uniformly sampled K_x -varying FEMs with their corresponding 2-DOF ICE ROMs. The force scaling factor f_r was randomized within the range of $[0.25, 0.75] \times \text{beam thickness}$ for each load case of each training FEM, so that the GPR ROM could also evaluate the uncertainty of the nonlinear ROM coefficients with respect to the load level on the FEMs [37]. Then, 900 uniformly sampled test sets of FEMs were tested on the trained GPR ROM to evaluate the predicted mean and its confidence interval of each ROM coefficient for the varying boundary stiffness. The predicted means and the confidence intervals for the cubic ROM coefficients are shown in Figure 3. The cubic coefficients accurately captured the smooth transition from the soft to stiff axial spring stiffness. This also reveals that 20 training samples were sufficient enough for the GPR ROM to capture the FEM variation with very small uncertainty. More details of the GPR ROM evaluation for the flat beam can be further found in [37].

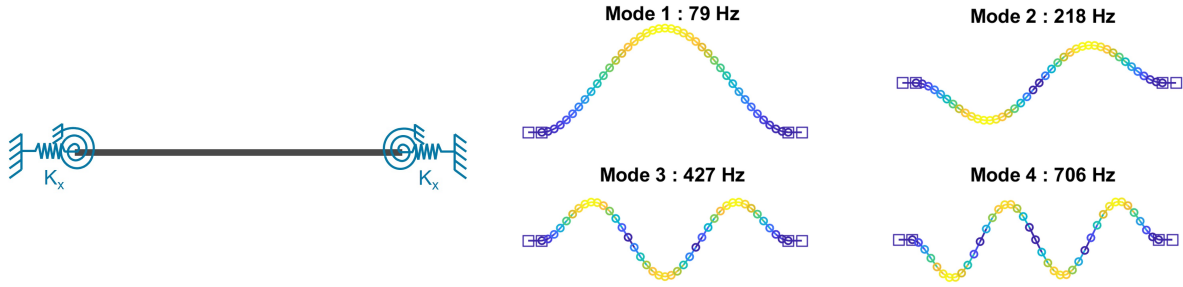


Figure 2: Schematic of the flat beam with boundary axial spring and its first four bending modes. The modes were computed with the nominal beam with maximum axial spring stiffness $K_{x,\max}$. (The figures are reprinted from [37].)

Modal basis in GPR ROM	Mode 1 & 3
Number of training sets (N_{tr})	20
Number of load cases per a training set (N_{nl})	7
Random force scaling range ($[f_{\min}, f_{\max}]$)	$[0.25, 0.75] \times \text{beam thickness}$
Number of test sets (N_{te})	900

Table 1: The GPR ROM training parameters for the flat beam model.

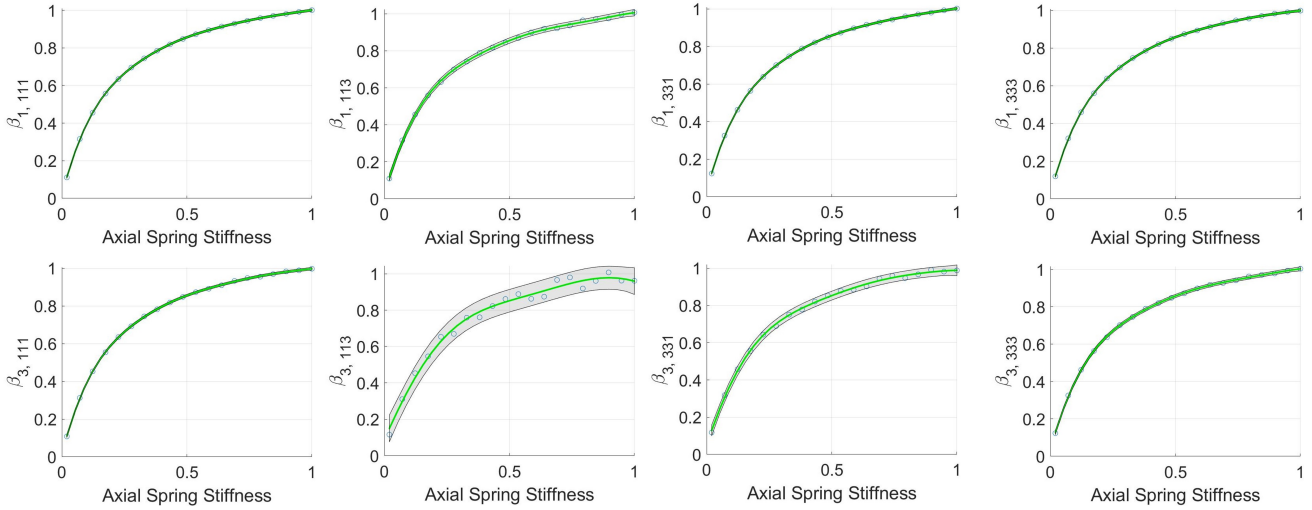


Figure 3: The GPR ROM prediction for the cubic ROM coefficients of the flat beam: trained observations (blue circles), mean prediction (green curve), and its 95% confidence interval (grey surface). The ROM coefficients and axial stiffness are all normalized by the nominal values. (The figures are reprinted from [37].)

3.2 GPR ROM based Model Updating of Flat Beam using NNMs

A target (or true) FEM used in this numerical study was chosen to have a boundary stiffness $K_{x,t} = 2.0 \times 10^5 \text{ lbf in}^{-1}$, while all the other parameters had the nominal values. Two initial FEMs with different design parameter values $K_{x,0} = 4.0 \times 10^5$ and $0.5 \times 10^5 \text{ lbf in}^{-1}$ were then used as initial guesses, and in each case the proposed GPR ROM based updating scheme was used to update the model to match the target NNM. Figure 4 shows the 1st NNMs computed from the target FEM and the two initial FEMs. In this case study, the state variable vector \mathbf{z} consisted of points on the 1st NNM represented by the frequency and transverse displacement of the center node of the beam.

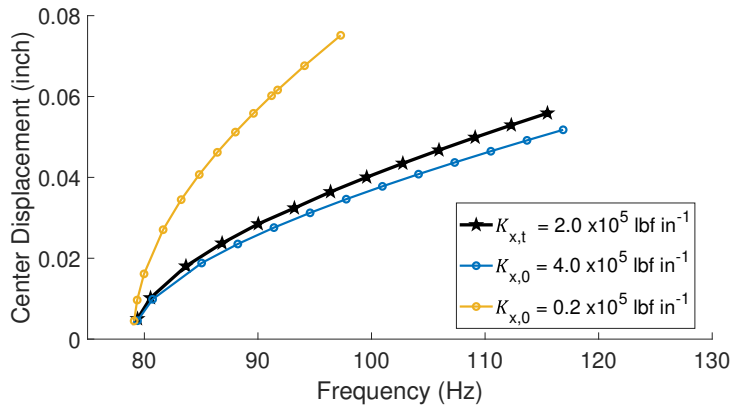


Figure 4: The 1st NNM curves of the target and initial flat beam models. The curves are computed by the MHB method using five harmonics.

Figure 5 shows how the NNMs of the initial models converge to the target NNM during the model updating routine. The initial and final parameter values as well as the cost function values are also presented in Table 2. The results show that the NNMs of both cases converged to the target NNM within a small number of iterations. The final cost function values were relatively small and the updated boundary stiffness values were also quite near to the target value. It can be inferred that the analytical sensitivity enabled the design variable to quickly find the optimal path to the true solution. It is also important to note that the GPR ROM constructed a smooth manifold (i.e., a curve) for each ROM coefficient for the given range of the design variable, as depicted in Figure 3. This information serves as a useful indicator that the optimization would be smooth and reliable as long as the FEM parameter and corresponding ICE ROM remain in the convex manifold.

The computational cost of the proposed model updating procedure was compared with a conventional FE model updating (FEMU) approach, which directly computes and correlates NNMs using a full FEM [38]. The computations were performed on an Intel Core i7-7700K 4.2GHz quad-core computer with 64 GB of RAM, and the results are presented in Table 3. The computational overhead for computing an NNM curve and its gradients was dramatically reduced by two to three orders of magnitude. The conventional FEMU, which also computes the NNMs using the MHB method, needed to find the numerical sensitivities of full linear matrices of mass and stiffness as the FEM parameters update. On the other hand, the proposed approach simply computed the analytical sensitivity, which is far more efficient to evaluate.

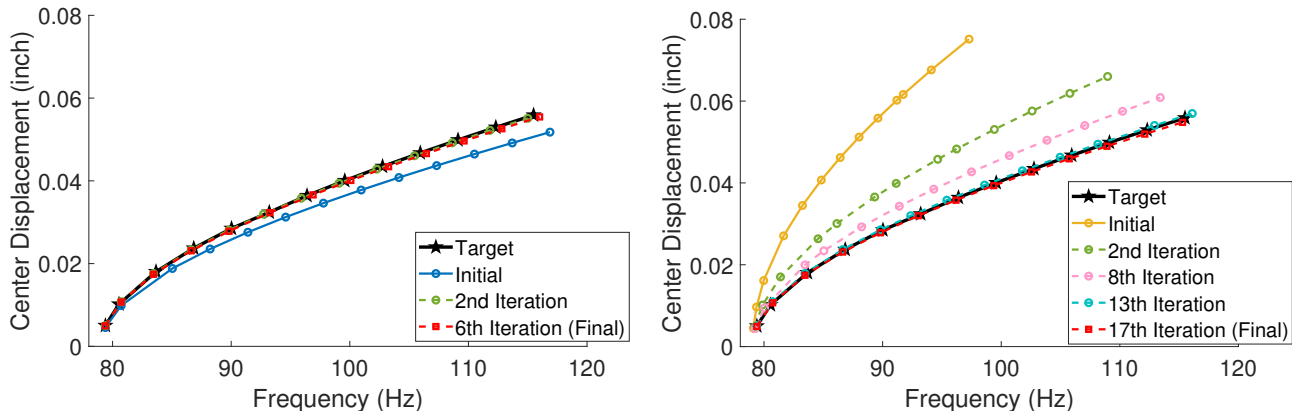


Figure 5: The 1st NNMs of the flat beam model at a few iterations of the model updating procedure. The 1st NNM curves of the FE models with $K_{x,0} = 4.0 \times 10^5$ (left) and $K_{x,0} = 0.2 \times 10^5$ lbf in⁻¹ (right).

Initial Parameter Values ($K_{x,0}$)	4.0000×10^5	0.2000×10^5
Initial Cost Function Value	3.3309×10^{-4}	0.4475
Final Parameter Value ($K_{x,0}$)	2.1204×10^5	2.1219×10^5
Final Cost Function Value	9.1943×10^{-6}	1.0263×10^{-5}
Number of Iterations	6	17

Table 2: The model updating results of the beam models with $K_{x,0} = 4.0 \times 10^5$ (left) and $K_{x,0} = 0.2 \times 10^5$ lbf in⁻¹ (right).

	Conventional FEMU	GPR ROM based FEMU
NNM computation	110.3172	0.6376
Gradient ($\frac{\partial x}{\partial p}$) computation	169.2634	0.0834

Table 3: The computational time comparison (s) between the conventional FEMU method in [38] and the proposed model updating method.

4 Conclusion

In this work, a GPR ROM based model updating method was developed, which could efficiently overcome some major challenges of the existing FEMU and ROMU approaches. The numerical example showed that, using the proposed framework, the FEM parameter quickly converged from its initial guess to the true value. This was because the computational cost required to estimate the NNMs and their gradients was greatly reduced, which are needed at each step in the model updating process. Compared to the ROMU approach in [35], the physical parameters were directly updated, and the number of design variables was kept relatively small. (There would have been 14 design variables if the ROMU approach in [35] were used.)

The proposed method was significantly fast in correlating the FEM parameters to match the target NNMs. This can be appealing in practice for updating nonlinear structural models, because one typically wants to run as many trials as needed to sort out the uncertain design parameters, and also to collect multiple possible solutions that correlate the models with actual experimental data.

The proposed approach achieves a very efficient model correlation at the cost of preparing a well-trained data-driven ROM. A simple structural model such as the flat beam could retain a small number of modes in a GPR ROM, and hence one could compute an accurate and convex GP model for each ROM coefficient with a small number of training samples. The optimization could then easily converge to the target by finding an optimal path on the smooth ROM manifolds. When the proposed method is applied to more complicated structures, such as curved plates, the GPR ROM may require more careful training, such as additional post-processing that detects the discontinuous variation of the ROM coefficients and regroups each of the continuous variations into separate subgroups. In this respect, a GPR ROM can serve as a useful gauge that evaluates the effect of the variation of the FEM parameters on the static/dynamic behaviors of the nonlinear structural model. This can further be used to judge whether the model correlation using that FEM parameter set will converge or not in the given uncertain parameter range.

One important aspect of the GPR ROM is that it can filter out uncertain or redundant nonlinear ROM coefficients as studied in [37]. It is expected that by neglecting the uncertain coefficients in the GPR ROM, the ROM prediction as well as its gradient with respect to FEM parameters will become more certain and accurate, consequently enhancing the quality of the model updating procedure. The effect of GPR ROM coefficient filtering on the proposed updating method will be examined as a future work.

In addition, the proposed GPR ROM based model updating will be tested to correlate a beam model to an actual 3D printed beam structure using experimentally measured NNMs. The proposed approach will also be applied to more complicated structures to validate its efficacy.

References

- [1] Eric J Tuegel, Anthony R Ingraffea, Thomas G Eason, and S Michael Spottswood. Reengineering aircraft structural life prediction using a digital twin. *International Journal of Aerospace Engineering*, 2011, 2011.
- [2] Edward Glaessgen and David Stargel. The digital twin paradigm for future nasa and us air force vehicles. In *53rd AIAA/ASME/ASCE/AHS/ASC Structures, Structural Dynamics and Materials Conference 20th AIAA/ASME/AHS Adaptive Structures Conference 14th AIAA*, page 1818, 2012.
- [3] Benjamin Smarslok, Adam Culler, and Sankaran Mahadevan. Error quantification and confidence assessment of aerothermal model predictions for hypersonic aircraft. In *53rd AIAA/ASME/ASCE/AHS/ASC Structures, Structural Dynamics and Materials Conference 20th AIAA/ASME/AHS Adaptive Structures Conference 14th AIAA*, page 1817, 2012.
- [4] Jacob D Hochhalter, William P Leser, John A Newman, Edward H Glaessgen, Vipul K Gupta, Vesselin Yamakov, Stephen R Cornell, Scott A Willard, and Gerd Heber. *Coupling Damage-Sensing Particles to the Digital Twin Concept*. National Aeronautics and Space Administration, Langley Research Center, 2014.
- [5] KD Murphy, LN Virgin, and SA Rizzi. Experimental snap-through boundaries for acoustically excited, thermally buckled plates. *Experimental Mechanics*, 36(4):312–317, 1996.
- [6] Chuh Mei, K. Abdel-Motagaly, and R. Chen. Review of Nonlinear Panel Flutter at Supersonic and Hypersonic Speeds. *Applied Mechanics Reviews*, 52(10):321–332, 10 1999.
- [7] DM Van Wie, DG Drewry, DE King, and CM Hudson. The hypersonic environment: required operating conditions and design challenges. *Journal of Materials Science*, 39(19):5915–5924, 2004.
- [8] John E Mottershead and MI Friswell. Model updating in structural dynamics: a survey. *Journal of sound and vibration*, 167(2):347–375, 1993.
- [9] Gaetan Kerschen, Keith Worden, Alexander F Vakakis, and Jean-Claude Golinval. Past, present and future of nonlinear system identification in structural dynamics. *Mechanical systems and signal processing*, 20(3):505–592, 2006.
- [10] Michael Friswell and John E Mottershead. *Finite element model updating in structural dynamics*, volume 38. Springer Science & Business Media, 2013.
- [11] Dennis Göge. Automatic updating of large aircraft models using experimental data from ground vibration testing. *Aerospace science and technology*, 7(1):33–45, 2003.
- [12] Tshildizi Marwala and Sibusiso Sibisi. Finite element model updating using bayesian framework and modal properties. *Journal of Aircraft*, 42(1):275–278, 2005.

- [13] Simon Peter, Alexander Grundler, Pascal Reuss, Lothar Gaul, and Remco I Leine. Towards finite element model updating based on nonlinear normal modes. In *Nonlinear Dynamics, Volume 1*, pages 209–217. Springer, 2016.
- [14] Mingming Song, Ludovic Renson, Jean-Philippe Noël, Babak Moaveni, and Gaetan Kerschen. Bayesian model updating of nonlinear systems using nonlinear normal modes. *Structural Control and Health Monitoring*, 25(12):e2258, 2018.
- [15] Chris I VanDamme, Matthew Allen, and Joseph J Hollkamp. Nonlinear structural model updating based upon nonlinear normal modes. In *2018 AIAA/ASCE/AHS/ASC Structures, Structural Dynamics, and Materials Conference*, page 0185, 2018.
- [16] Gaëtan Kerschen, Maxime Peeters, Jean-Claude Golinval, and Alexander F Vakakis. Nonlinear normal modes, part i: A useful framework for the structural dynamicist. *Mechanical Systems and Signal Processing*, 23(1):170–194, 2009.
- [17] Maxime Peeters, Régis Vigié, Guillaume Sérandour, Gaëtan Kerschen, and J-C Golinval. Nonlinear normal modes, part ii: Toward a practical computation using numerical continuation techniques. *Mechanical systems and signal processing*, 23(1):195–216, 2009.
- [18] David A Ehrhardt and Matthew S Allen. Measurement of nonlinear normal modes using multi-harmonic stepped force appropriation and free decay. *Mechanical Systems and Signal Processing*, 76:612–633, 2016.
- [19] Joseph D Schoneman, Matthew S Allen, and Robert J Kuether. Relationships between nonlinear normal modes and response to random inputs. *Mechanical Systems and Signal Processing*, 84:184–199, 2017.
- [20] Alexander A Muravyov and Stephen A Rizzi. Determination of nonlinear stiffness with application to random vibration of geometrically nonlinear structures. *Computers & Structures*, 81(15):1513–1523, 2003.
- [21] Ricardo Perez, XQ Wang, and Marc P Mignolet. Nonintrusive structural dynamic reduced order modeling for large deformations: enhancements for complex structures. *Journal of Computational and Nonlinear Dynamics*, 9(3), 2014.
- [22] MI McEwan, Jan R Wright, Jonathan E Cooper, and Andrew Yee Tak Leung. A combined modal/finite element analysis technique for the dynamic response of a non-linear beam to harmonic excitation. *Journal of Sound and Vibration*, 243(4):601–624, 2001.
- [23] M McEwan, J Wright, J Cooper, and A Leung. A finite element/modal technique for nonlinear plate and stiffened panel response prediction. In *19th AIAA Applied Aerodynamics Conference*, page 1595, 2001.
- [24] Joseph J Hollkamp, Robert W Gordon, and S Michael Spottswood. Nonlinear modal models for sonic fatigue response prediction: a comparison of methods. *Journal of Sound and Vibration*, 284(3-5):1145–1163, 2005.
- [25] Joseph J Hollkamp and Robert W Gordon. Reduced-order models for nonlinear response prediction: Implicit condensation and expansion. *Journal of Sound and Vibration*, 318(4-5):1139–1153, 2008.
- [26] Johannes B Rutzmoser, Daniel J Rixen, Paolo Tiso, and Shobhit Jain. Generalization of quadratic manifolds for reduced order modeling of nonlinear structural dynamics. *Computers & Structures*, 192:196–209, 2017.
- [27] Morteza Karamooz Mahdiabadi, Paolo Tiso, Antoine Brandt, and Daniel Jean Rixen. A non-intrusive model-order reduction of geometrically nonlinear structural dynamics using modal derivatives. *Mechanical Systems and Signal Processing*, 147:107126, 2021.
- [28] Cyril Touzé, Olivier Thomas, and Antoine Chaigne. Hardening/softening behaviour in non-linear oscillations of structural systems using non-linear normal modes. *Journal of Sound and Vibration*, 273(1-2):77–101, 2004.
- [29] Cyril Touzé and M Amabili. Nonlinear normal modes for damped geometrically nonlinear systems: Application to reduced-order modelling of harmonically forced structures. *Journal of sound and vibration*, 298(4-5):958–981, 2006.
- [30] George Haller and Sten Ponsioen. Nonlinear normal modes and spectral submanifolds: existence, uniqueness and use in model reduction. *Nonlinear dynamics*, 86(3):1493–1534, 2016.
- [31] Robert Szalai, David Ehrhardt, and George Haller. Nonlinear model identification and spectral submanifolds for multi-degree-of-freedom mechanical vibrations. *Proceedings of the Royal Society A: Mathematical, Physical and Engineering Sciences*, 473(2202):20160759, 2017.

- [32] Marc P Mignolet, Adam Przekop, Stephen A Rizzi, and S Michael Spottswood. A review of indirect/non-intrusive reduced order modeling of nonlinear geometric structures. *Journal of Sound and Vibration*, 332(10):2437–2460, 2013.
- [33] Cyril Touzé, Alessandra Vizzaccaro, and Olivier Thomas. Model order reduction methods for geometrically nonlinear structures: a review of nonlinear techniques. *Nonlinear Dynamics*, 105(2):1141–1190, 2021.
- [34] Vivien Denis, M Jossic, Christophe Giraud-Audine, B Chomette, A Renault, and Olivier Thomas. Identification of nonlinear modes using phase-locked-loop experimental continuation and normal form. *Mechanical Systems and Signal Processing*, 106:430–452, 2018.
- [35] Christopher I Van Damme, Matthew S Allen, and Joseph J Hollkamp. Updating geometrically nonlinear reduced-order models using nonlinear modes and harmonic balance. *AIAA Journal*, pages 1–16, 2020.
- [36] Kyusic Park and Matthew S Allen. Tuning of finite element model parameters to match nonlinear reduced order models. In *Nonlinear Structures & Systems*, volume 1, pages 113–116. Springer, 2021.
- [37] Kyusic Park. *Data-driven Reduced Order Modeling and Model Updating of Geometrically Nonlinear Structures*. PhD thesis, Brigham Young University, 2022.
- [38] Christopher I VanDamme. *Model Correlation and Updating of Geometrically Nonlinear Structural Models Using Nonlinear Normal Modes and the Multi-Harmonic Balance Method*. PhD thesis, The University of Wisconsin-Madison, 2019.
- [39] Christopher KI Williams and Carl Edward Rasmussen. *Gaussian processes for machine learning*, volume 2. MIT press Cambridge, MA, 2006.
- [40] Carl Edward Rasmussen. Advanced lectures on machine learning. *Gaussian Processes in Machine Learning*, pages 63–71, 2004.
- [41] Thibaut Detroux, Ludovic Renson, Luc Masset, and Gaëtan Kerschen. The harmonic balance method for bifurcation analysis of large-scale nonlinear mechanical systems. *Computer Methods in Applied Mechanics and Engineering*, 296:18–38, 2015.
- [42] Richard H Byrd, Jean Charles Gilbert, and Jorge Nocedal. A trust region method based on interior point techniques for nonlinear programming. *Mathematical programming*, 89(1):149–185, 2000.